

The Birthplaces of Gamma-Ray Bursts

Patrick A. Young^{1,2} & Chris L. Fryer^{3,4}

ABSTRACT

We use population synthesis to construct distributions of gamma-ray bursts (GRBs) for different proposed progenitor models. We use a description of star formation that takes into account the evolution of metallicity with redshift and galaxy mass, the evolution of galaxy mass with redshift, and the star formation rate with galaxy mass and redshift. We compare predicted distributions with redshift and metallicity to observations of GRB host galaxies and find that the simple models cannot produce the observed distributions, but that current theoretical models can reproduce the observations within some constraints on the fraction of fallback black holes that produce GRBs.

Subject headings: Gamma Rays: Bursts, Supernovae: General

1. Introduction

With the advent of the SWIFT satellite the number of gamma-ray bursts (GRBs) with multiwavelength observations of afterglows and host galaxies is growing rapidly. As the data increases, it has the potential to allow us to probe deeper into the question of the progenitors of these outbursts. On the surface, much of the data seems contradictory (for a review, see Fryer et al. (2007)): recent data has confirmed that the explosions behind long-duration bursts produce supernovae, but we now know that some don't, or if they do, they produce dim supernovae (Fynbo et al. 2006; Berger et al. 2006); GRBs are associated with star forming regions, but they appear to occur in lower mass galaxies than their supernova counterparts (Fruchter et al. 2006); and although many bursts occur at metallicities below 1/10th solar, the average metallicity of bursts may well be closer to 1/3 to 1/2 solar (Prochaska 2007).

All of this data may not be as contradictory as it seems. For instance, the idea that many bursts occur in low metallicity environments need not mean that bursts are exclusively produced by low-metallicity stars. If we consider that star formation is biased towards higher redshift and lower mass galaxies than a typical L^* galaxy today, both of which imply lower metallicities, we might expect such an observational bias even if there is *no* metallicity dependence for GRB progenitors at all. As our sample of well-studied bursts grows, it will become easier to extract reality from observational bias.

Theory has long made qualitative predictions about these bursts. Bursts are believed to come from black hole forming stars and the stars that form black holes tend to be the most massive stars. Thus, it is not surprising that GRBs and supernovae do not occur in exactly the same conditions. Since the strong stellar winds seen at high metallicities will prevent stars from collapsing directly to black holes, it has long been

¹Astronomy Department, The University of Arizona, Tucson, AZ 85721

²X Division, Los Alamos National Laboratory, Los Alamos, NM 87545

³Department of Physics, The University of Arizona, Tucson, AZ 85721

⁴CCS Division, Los Alamos National Laboratory, Los Alamos, NM 87545

suggested the rate of long duration bursts will be higher at lower metallicities (Fryer, Woosley & Hartmann 1999; Fryer et al. 2007). Because the ^{56}Ni yield of a GRB explosion depends sensitively on whether the black hole is formed directly or by fallback in a weak initial explosion, theorists have also known that bursts would not necessarily always be accompanied by bright supernova outbursts (Fryer, Woosley & Hartmann 1999; Fryer et al. 2006b). But to actually extract information about GRB progenitors with the current data, we must develop a more quantitative theory.

In this paper we perform population synthesis calculations to determine if the common progenitor scenarios for long duration GRBs can be distinguished based upon the observational data. We combine the star formation rate as a function of redshift, evolution of cosmic metal density with redshift, the mass metallicity relation for galaxies, and the specific star formation rate versus galaxy mass. Using a Monte Carlo technique, we sample these distributions to produce the expected population of gamma-ray bursts and supernovae as a function of metallicity, redshift, and even host galaxy mass. Depending upon the progenitor, these distributions differ and we can use observations of bursts to constrain the progenitor model.

Section 2 describes the population synthesis Monte Carlo code used to create the simulated distributions, the descriptions of star formation and host galaxy properties used, and the GRB progenitor models. Section 3 compares our simulated distributions to observed GRB rates. Section 4 discusses the implications for the nature of GRB progenitors and our ability to constrain theoretical models.

2. Calculations

2.1. Initial Conditions

We calculate the observed population of gamma-ray bursts by introducing a Monte-Carlo code that pulls from a sample of stars based on what we know of star formation. The fate of a massive star depends upon its metallicity, its initial mass, and its initial spin. To calculate the distribution of gamma-ray bursts, we first must assume a distribution for each of these quantities.

Since the average metallicity of the universe decreases with increasing redshift, the metallicity of our entire distribution of GRBs clearly depends upon the star formation rate as a function of redshift. The mass-metallicity relation for galaxies also requires that we take into account the mass distribution of galaxies with redshift and the star formation rate as a function of galaxy mass.

For our simple model, we use the functional form of the star formation rate per unit volume as a function of redshift (z) from Watanabe et al.(1999)

$$\log[\eta(z)] = \begin{cases} A \log(1+z) & \text{for } z \leq z_p \\ A \log(1+z_p) - B(z-z_p) & \text{for } z > z_p \end{cases} \quad (1)$$

A, B, z_p are parameters that describe the star formation rate. The star formation rises from the initial burst of star formation and peaks at z_p and then drops precipitously as we approach redshift of 0. Our standard model for the star formation history is based on a fit of this simple model to the current observations (including the metallicity evolution we use based on the work of Hopkins & Beacom 2006 - see below): $(A, B, z_p) = (1.0, 0.5, 2.5)$. The star formation history remains uncertain, but its peak is now believed to lie somewhere between 2 and 3. We run 2 additional models probing the dependence of our results on this history: $(A, B, z_p) = (1.25, 0.5, 2.0)$ and $(1.0, 0.1, 2.5)$. To get the rate of star formation in a given redshift

bin, we must also correct for the volume filling factor:

$$\Delta V(z) = \Delta z(1.0 - \sqrt{1.0 + z})^2 \times (1.0 + z)^{-3/2}. \quad (2)$$

For the mass-metallicity relation for galaxies we use the prescription derived by Tremonti et al. (2004) from the Sloan Digital Sky Survey (SDSS) galaxy sample, which has the functional form

$$12 + \log(\text{O}/\text{H}) = -1.492 + 1.847 \log M_* - 0.08026(\log M_*)^2 \quad (3)$$

Erb et al. (2006) show that the shape of the mass-metallicity relation remains essentially the same out to redshifts of $z \sim 2$, varying primarily in the normalization of the total metal content. We assume that the total metallicity scales along with the $\log(\text{O}/\text{H})$ ratio. This is of course not strictly true, but it is the best observational approximation available. We assume that this functional form is valid to higher redshifts and shift the normalization of the distribution according to the total metal density of the universe as a function of redshift. For the total metal density we adopt the form in Hopkins & Beacom (2006).

$$\dot{\rho}_* = (a + bz)/[1 + (z/c)^d] h_{70} M_\odot yr^{-1} Mpc^{-3} \quad (4)$$

$$\dot{\rho}_* = 63.7 \dot{\rho}_z \quad (5)$$

$$\rho_z(z) = \int^z \dot{\rho}_z dz \quad (6)$$

where $\dot{\rho}_*$ is the rate of change of the stellar mass density with redshift, $\dot{\rho}_z$ is the rate of change of the metal density, and the coefficients $a = 0.017$, $b = 0.13$, $c = 3.3$ and $d = 5.3$ are defined in Cole et al. (2001).

We use the galaxy mass function for $z \leq 4$ from the GOODS-MUSIC sample (Fontana et al. 2006). This is fit with a Schechter function with redshift dependent M_* , and α_* described as described in Fontana et al. (2006):

$$f(M_{\text{galaxy}}) \propto \log[10^{M-M^*(z)}]^{\alpha^*(z)} e^{-10^{M-M^*(z)}} \quad (7)$$

where M is the log of the galaxy mass, $M^*(z) = 11.16 + 0.17z - 0.07z^2$, and $\alpha^*(z) = -.18 - 0.082z$. Above a redshift of 4, we set the mass function to the value at a redshift of 4.

The most difficult part of the problem is a description for the star formation rate as a function of galaxy mass at different redshifts. The star formation in the local universe is dominated by dwarf galaxies, but by redshifts of 0.7 large spirals account for more than half. We produce a rough estimate of the specific star formation rate (\dot{M}_\odot/M_*) with respect to galaxy mass from Figure 13 of Papovich et al. (2006). We fit a line to the points in the figures and take this as the specific star formation rate in three redshift bins centered on the redshifts of the three panels of their Figure 14:

$$\log(SFR/M_{\text{galaxy}}) \propto 1.035 \log M_{\text{galaxy}} \text{ if } z < 0.5 \quad (8)$$

$$\propto 0.8947 \log M_{\text{galaxy}} \text{ if } 0.5 < z < 0.7 \quad (9)$$

$$\propto 0.44 \log M_{\text{galaxy}} \text{ if } 1.5 < z \quad (10)$$

where M_{galaxy} is the galaxy mass. These approximations are crude, but at least give us a zeroth order correction to the metallicity distribution of GRBs due to the mass-metallicity relation.

For our simple stellar mass distribution, we assume a single power law on the mass (M) of the star:

$$f(M) = M^{-\Gamma} dM, \quad (11)$$

where Γ is set to 2.7 for our baseline case.

At this point, the uncertainties in our understanding of the evolution of angular momentum is too great for us to make any calculations of this quantity. For the time being, we assume that there is always sufficient angular momentum to make a GRB. This provides an upper limit on the GRB rate.

2.2. Fates of Systems

With the initial conditions outlined above, we produce a population of stars with given metallicities. To determine which is a GRB, we must then convolve this result with our knowledge of stellar evolution. Unfortunately, the final state of a star differs for different stellar evolution codes. The primary physical uncertainties in these codes include our understanding of convection in the stars (especially when it is coupled to nuclear burning), pulsational instabilities, and mass loss. Understanding rotation adds a new layer of uncertainties and we will not study this further in the paper. Binary stellar models are few and far between, generally focusing on specific objects. We will only make rough estimates of binary progenitors in this paper.

As a test case, we first introduce a simple model that assumes all stars above a certain mass limit produce GRBs. This ignores the fact that mass loss is required to remove the hydrogen envelope, and too much mass loss prevents the formation of a black hole. We will use this simple model as a gauge to test our more realistic progenitor scenarios: basic single star progenitors, binary star progenitors, and the more recent single-star models suggested by Yoon & Langer (2005).

For our basic single-star models, we take the Heger et al. (2003) paper using the strict definition of the plots where the metallicity is given as a log plot with “about solar” taken for exactly solar and the lower part of the plot taken for 10^{-6} solar. Using these definitions, we can predict the fates of a star as a function of metallicity and mass. Recall that our minimum requirements for a GRB are that the star must (i) collapse down to form a black hole and (ii) lose its hydrogen envelope¹.

Our estimate of the effects of binaries is to assume that binary systems always remove the hydrogen envelope of the collapsing star. So our constraint for making GRBs is simply that the star must collapse to a black hole. Here we still use the Heger et al.(2003) distribution, but we can now extend the formation to include those stars that would normally still retain a hydrogen envelope. Note that specific binary scenarios may well produce distributions that are very different than the one used in our simple choice, but this provides us with a first guess of the distribution.

We also include the more recent model suggested by Yoon & Langer (2005) that found that high rotation in stars could lead to extensive mixing that allows the near-complete burning of the hydrogen envelope. We base our models on the predictions in their most recent results(Yoon et al. 2006).

Finally, remember that we can form black holes in 2 separate ways: a direct collapse to a black hole or the delayed collapse to a black hole via fallback after a weak supernova explosion. Some fraction of weak

¹We assume that the star has sufficient angular momentum to form a GRB in all cases and hence, all our GRB rates are upper limits. We discuss the repercussions of this assumption more fully in the conclusions.

supernova explosions will form very little ^{56}Ni (Fryer et al. 2006) and we will differentiate between these two black hole formation mechanisms.

3. Results

For most of our studies, we will use the classic single GRB rate as the basis for our intuition. Figure 1 shows the fraction of total outbursts per $\Delta z = 0.1$ bin for 5 types of explosion: Type II supernovae, Weak Type II supernovae, Type Ib/c Supernovae, Weak Type Ib/c supernovae, and Direct-Collapse GRBs. The weak supernovae will produce black holes. For single stars, the weak Type Ib/c supernovae may also produce GRBs. The binary rate is very similar except that binaries can eject the hydrogen envelopes of the primary star, producing more Type Ib/c supernovae, and hence, more potential GRB systems through fallback. Note that the peak GRB rate from direct collapse happens at a higher redshift than core-collapse supernovae, but the weak supernovae are not so different than the redshift distribution of type II supernovae. Strong Type Ib/c supernovae have the lowest mean redshift.

We expect GRBs to be made up of both direct-collapse and fallback black holes, but determining which type of black hole formation scenario dominates the distribution is difficult to determine. First and foremost, we do not know exactly which stars have weak supernova explosions versus the number that have no explosion (Fryer 1999). Second, we know that fallback black holes will be less efficient than direct-collapse black holes at forming GRBs. This is because the accretion rate in a fallback black hole system is lower (possibly significantly lower) than a direct-collapse black hole system. The lower accretion rate, the weaker the power available to drive an explosion. Popham et al. (1999) argued that the accretion rate would have to be above $0.01 M_{\odot} y^{-1}$ to produce a GRB if it is powered by neutrinos². Recall also that the rates for GRBs here are upper limits (assuming all stars have enough angular momentum).

Figure 2 shows the metallicity of GRBs and supernovae versus redshift for 6 separate simulations. Note that without the fallback black holes, the metallicity distribution of single and binary stars under the Heger et al. (2003) model predicts essentially all bursts occur below a metallicity of 0.1, very similar to the Yoon et al. (2006) prediction. This is because the Heger et al. (2003) models argue that above this metallicity winds are sufficiently strong that massive stars only form black holes through fallback. With fallback black holes, metallicities can be nearly as high as the supernova distribution (indeed, at high redshift, single stars predict metallicities higher than the supernova rate). A simple explanation of any result that lies in between the pure direct-collapse and direct-collapse plus fallback systems is that the fraction of fallback black hole systems that form GRBs is smaller than those of direct-collapse black holes. Measuring this system could tell us about how fallback occurs in weak supernovae.

Figure 3 shows the metallicity distribution for our binary models for two separate star-formation histories. Although the flatter star formation history allows bursts and supernovae to occur at higher redshift, the other changes are fairly minimal. Only the highest redshift bursts will really help us constrain the star formation history.

Figure 4 shows the metallicity distribution of all explosions as a function of redshift. The total GRB distribution could be the summation of the direct-collapse and some fraction of weak Type Ib/c supernovae. Binary systems are similar, except that their distribution could include the direct collapse plus both types

²This constraint probably also exists for magnetically-driven outbursts at some level.

of weak supernovae. In any event, we expect the GRB population to have at least a slightly lower mean metallicity than supernovae. Included in Figure 4 is a plot assuming showing the combined distribution assuming 2% of all fallback black holes produce GRBs in the binary scenario. This produces a mean metallicity for GRBs just a little above 1/10th solar. This mean metallicity could be significantly lower if direct-collapse GRBs dominate the GRB rate. It is no surprise that the mean mass of GRB-producing galaxies is also lower than normal supernovae (Fig. 5).

Figure 6 shows the number of binary GRBs including those from weak SN II and Ib/c(top), single star GRBs including weak SN Ib/c (middle), and all supernovae (bottom) per $\Delta = 0.1$ bin in redshift and log metallicity ($\log(z/z_\odot)$), normalized to the number in the peak bin. Contours are plotted for bins with 20, 40, 60, and 80% of the peak number. On top of these contours, we show the current measurements of metallicity and redshift of GRBs associated damped Ly α absorbers available in the literature (Prochaska 2007). Triangles represent lower limits, circles metallicity estimates with error bars. The peaks of the predicted distributions are similar, but the GRBs have a much larger extent to low metallicities. This is greatest for the single star models. These models require the largest progenitor masses. As expected, the production of GRBs peaks between redshifts of 2 and 3, since that is where our star formation rate peaks.

Figure 7 shows the number of binary GRBs including those from weak SN II and Ib/c(top), single star GRBs including weak SN Ib/c (middle), and all supernovae (bottom) per $\Delta = 0.1$ bin in redshift and log of host galaxy stellar mass [$\log(M/M_\odot)$], normalized to the number in the peak bin. Contours are plotted for bins with 20, 40, 60, and 80% of the peak number. While the populations have similar peaks, a larger fraction of GRBs occur in sub-L* galaxies. The higher specific star formation rate in low mass galaxies produces IMFs populated all the way up to the high mass stars that produce GRBs, while high star formation rate massive galaxies do not populate the extreme masses as well, producing a larger volume of relatively poorer stellar populations. This bias also explains the bias towards low metallicity in GRB hosts, as lower mass galaxies also have a lower metal content.

Figure 8 shows contour plots similar to Figures 6 and 7 but for the “combined” scenario of Figure 4. By only including 2% of fallback black holes the peak of the distribution shifts to considerably lower metallicities and host galaxy masses. This distribution provides a reasonable approximation to the observed metallicity distribution.

4. Conclusions

In this paper, we present the theoretical distribution of GRBs as a function of redshift and of metallicity for the basic GRB models. We use current distributions of star formation, including the relative star formation rates of different-sized galaxies. In this manner, we can directly compare the predictions of the basic progenitor models to that of the growing set of observational data.

From figure 9, which shows the same observational data overplotted on figure 6, we can immediately see that the small sample of GRBs is definitely at odds with the predictions of our simple models. For instance, the unmodified Yoon & Langer scenario cannot account for all GRBs. Their model is unable to produce any significant number of GRBs above metallicities of 0.1 solar. If the metallicity of GRBs without firm determinations lie even modestly above their lower limits, then at least half the sample has metallicities above 0.1 solar. Similarly, direct black hole scenarios for both the binary and single star models are also biased towards low metallicity because mass loss at high metallicity is too extensive in the models. These models do have the advantage of producing a relatively flat metallicity distribution for low to moderate redshifts,

and there is no obvious trend of metallicity with redshift in the data.

Binary and single star models that include all fallback black holes produce too many GRBs at high metallicity by reducing the minimum mass for producing a GRB sufficiently that the GRB distribution to a large extent mimics the total supernova distribution. This also can be ruled out by the observations.

We can make our models fit the data by assuming that the relative fraction of GRBs from fallback black holes is roughly equal to that of direct collapse. This can occur either by arguing that only a small fraction of fallback black holes have accretion rates that are high enough to produce GRBs or by moving down the critical mass that delineates fallback black hole formation from direct collapse black hole formation. Either of these possibilities could easily be true, and unfortunately, at this time, theory has not made any definitive predictions on either of these.

Quantitative estimates of host galaxy mass are not available for a significant number of GRBs. However, we can examine morphologies and see that most GRBs occur in small, actively star forming galaxies with peculiar optical morphologies. This is consistent with a bias towards low mass hosts. Again, the fallback scenarios produce too many GRBs at high host galaxy mass, but a reduced fraction of fallback black holes could easily be made to fit the data.

There are several caveats to our current analysis. The first is that the current observed sample is still small and the observed distribution may change significantly when we have a larger statistical sample. Until the observational biases for the data we have can be understood and removed, it is dangerous to make any strong conclusions. In addition, we have made very simplistic models for the fates of massive stars. Binary progenitor models are much more complex than the simple models we have used, and until we have firm predictions from these models, it is difficult to make firm conclusions about these progenitors. Likewise, the most recent single-star models will evolve with time, and perhaps the inclusion of more complete physics will alter them to fit the data better. Fortunately, this framework can accommodate any progenitor prescription, so it can be used to test more sophisticated models as they become available.

Acknowledgments It is a pleasure to thank Aimee Hungerford and Jason Prochaska for useful discussions on this project. We also thank Jason Prochaska for providing his latest data on GRB metallicities. This project was funded in part under the auspices of the U.S. Dept. of Energy, and supported by its contract W-7405-ENG-36 to Los Alamos National Laboratory, and by a NASA grant SWIF03-0047.

REFERENCES

- Berger, E. et al. 2006, submitted to ApJ, astro-ph/0611128
- Cole, S. et al. 2001, MNRAS, 326, 255
- Erb, Dawn K., Shapley, Alice E., Pettini, Max, Steidel, Charles C., Reddy, Naveen A., & Adelberger, Kurt L. 2006, ApJ, 644, 813
- Fontana, A. et al. 2006, A&A, 459, 745
- Fruchter, A.S., Levan, A.J., Strolger, L., Vreeswijk, P.M. et al. 2006, Nature, 441, 463
- Fryer, C.L. 1999, ApJ, 522, 413
- Fryer, C.L., Woosley, S.E., & Hartmann, D. 1999, ApJ, 526, 152

- Fryer, Chris L., Young, Patrick A., & Hungerford, Aimee 2006, ApJ, 650, 1028
- Fryer et al. 2007, submitted to ApJ, astro-ph/
- Fynbo, J.P.U. et al., 2006, astro-ph/0608313
- Heger, A., Fryer, C.L., Woosley, S.E., Langer, N., Hartmann, D.H. 2003, ApJ, 591, 288
- Hopkins, Andrew M. & Beacom, John F. 2006, ApJ, 651, 142
- Limongi, M., & Chieffi, A. 2006, ApJ, 647, 483
- Papovich, C. et al. 2006, ApJ, 640, 92
- Popham, R., Woosley, S.E., & Fryer, C.L. 1999, ApJ, 518, 356
- Prochaska, Jason X. et al. 2007, ApJ, submitted
- Tremonti, Christy A. et al. 2004, ApJ, 613, 898
- Watanabe, K., Hartmann, D.H., Leising, M.D., & The, L.-S. 1999, ApJ, 516, 285
- Yoon, S.-C., & Langer, N. 2005, A&A, 443, 643
- Yoon, S.-C., Langer, N., & Norman, C. 2006, A&A, 460, 199

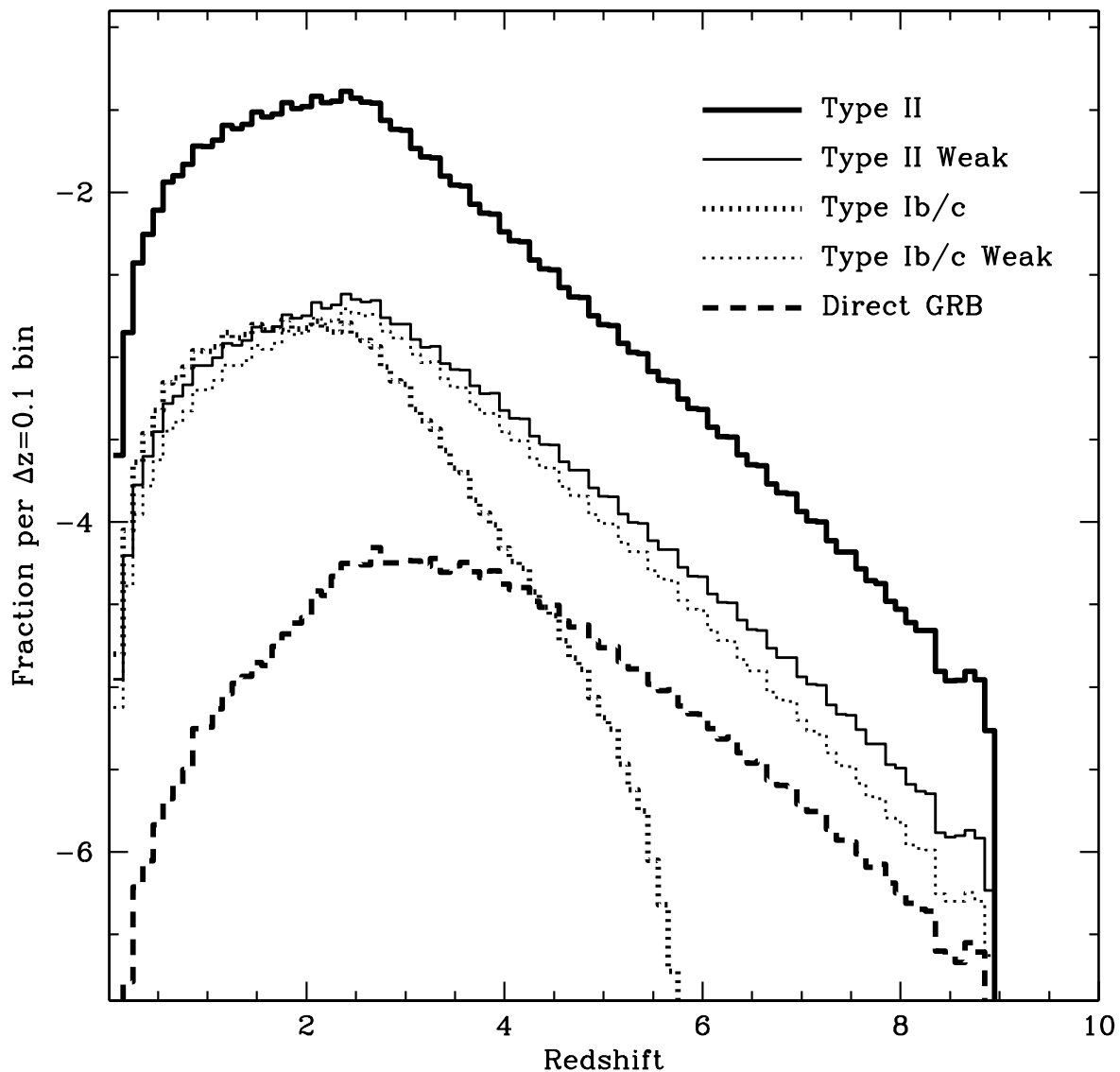


Fig. 1.— Fraction of total outbursts per $\Delta z = 0.1$ bin for 5 types of explosion: Type II supernova, Weak Type II supernova, Type Ib/c Supernova, Weak Type Ib/c supernova, Direct-Collapse GRB. The weak supernovae will produce black holes. Note that the GRB rate from direct collapse happens at a higher redshift than core-collapse supernovae, but the weak supernovae are not so different than the redshift distribution of type II supernovae. Strong Type Ib/c supernovae have the lowest mean redshift.

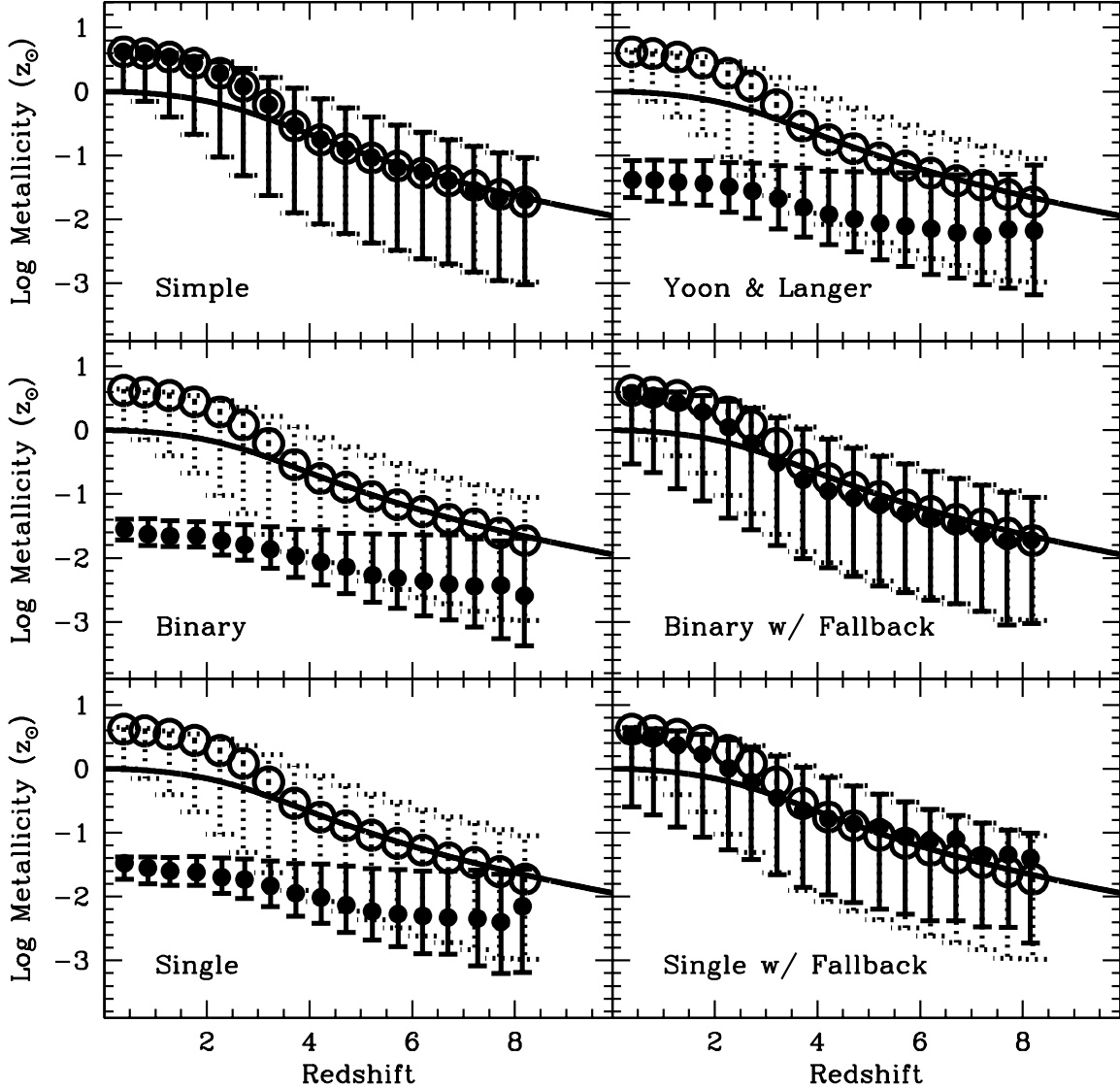


Fig. 2.— Metallicity of GRBs (solid circle and lines) and Supernovae (open circles and dotted lines) versus redshift for 6 separate simulations: our simple model using just a mass limit, the Yoon et al. (2006) model prediction, Single and Binary models with and without fallback black holes included. The error bars correspond to the range enclosing 90% of all bursts. The solid line shows the metallicity of an L^* galaxy as a reference point. Note that without the fallback black holes, the metallicity distribution of single and binary stars under the Heger et al. (2003) model predicts essentially all bursts occur below a metallicity of 0.1, very similar to the Yoon et al. (2006) prediction. But with fallback black holes, metallicities can be nearly as high as the supernova distribution (indeed, at high redshift, single stars predict metallicities higher than the supernova rate).

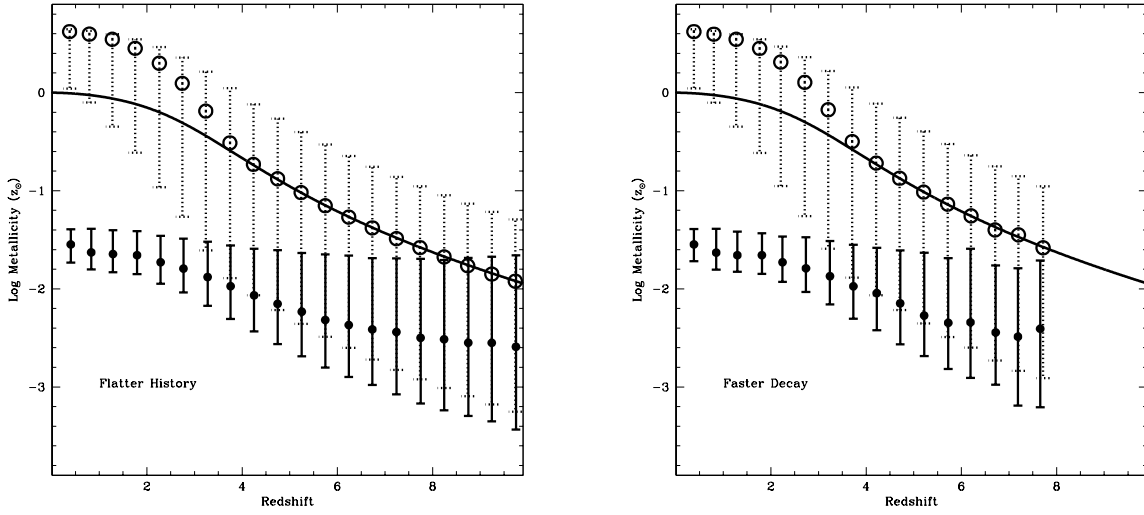


Fig. 3.— The metallicity distribution as a function of redshift for our direct-collapse binary GRBs and supernovae using two different star formation histories: A, B, z_p from equation 1 are (1.25, 2.0, 0.5) and (1.0, 2.5, 0.1) for the decay and flat histories respectively. Within these narrow bounds of the star formation history, the changes in the history are modest.

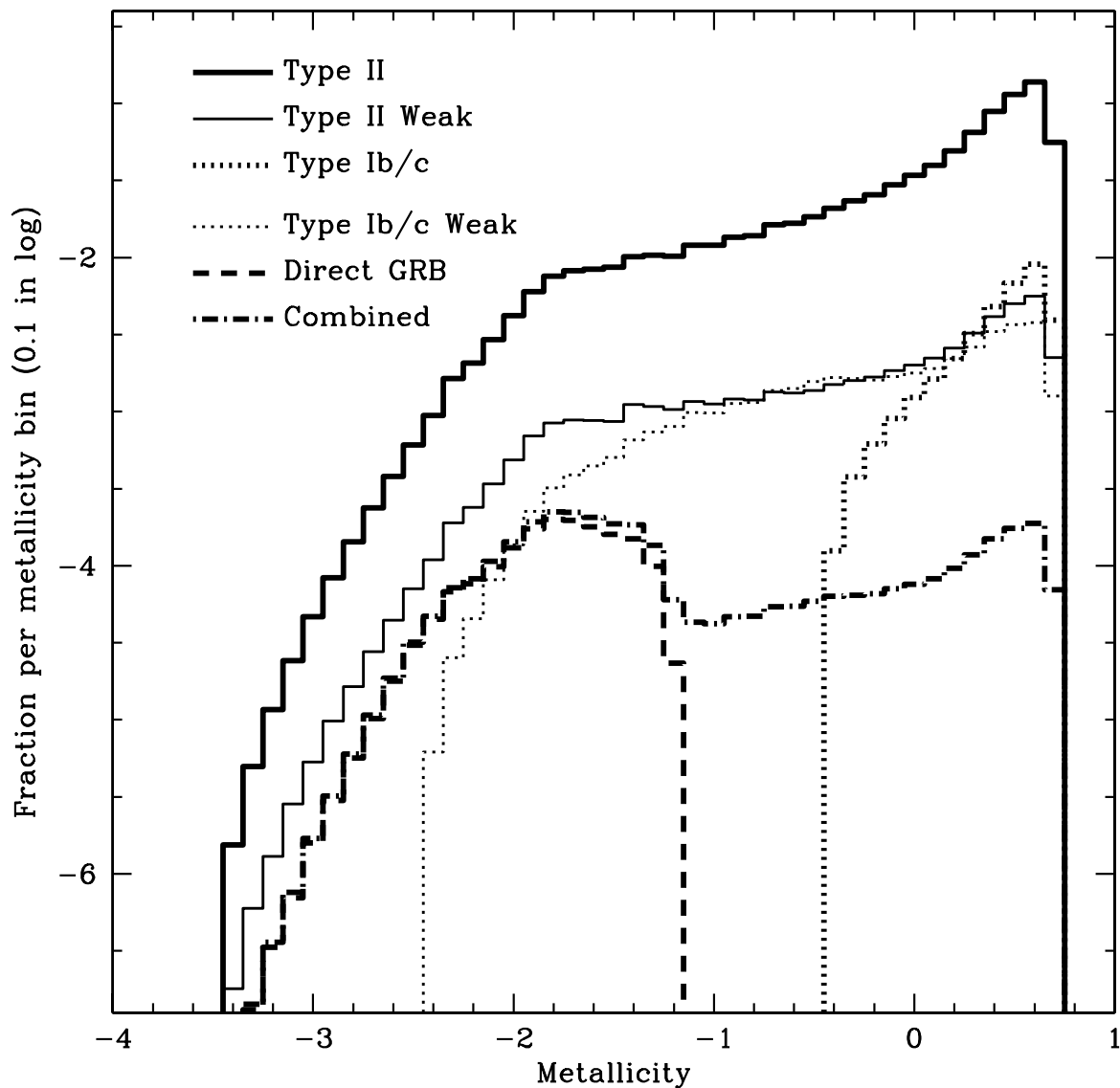


Fig. 4.— Fraction of explosions per metallicity bin (0.1 in log space) as a function of metallicity for single stars. The total GRB distribution could be the summation of the direct-collapse and weak Type Ib/c supernovae. “Combined” is the sum of the direct collapse and 2% of the weak Type Ib/c rate. Binary systems are nearly identical, except that their distribution could include the direct collapse plus both types of weak supernovae. In any event, we expect the GRB population to have at least a slightly lower mean metallicity than supernovae. This mean metallicity could be significantly lower if direct-collapse GRBs dominate the GRB rate.

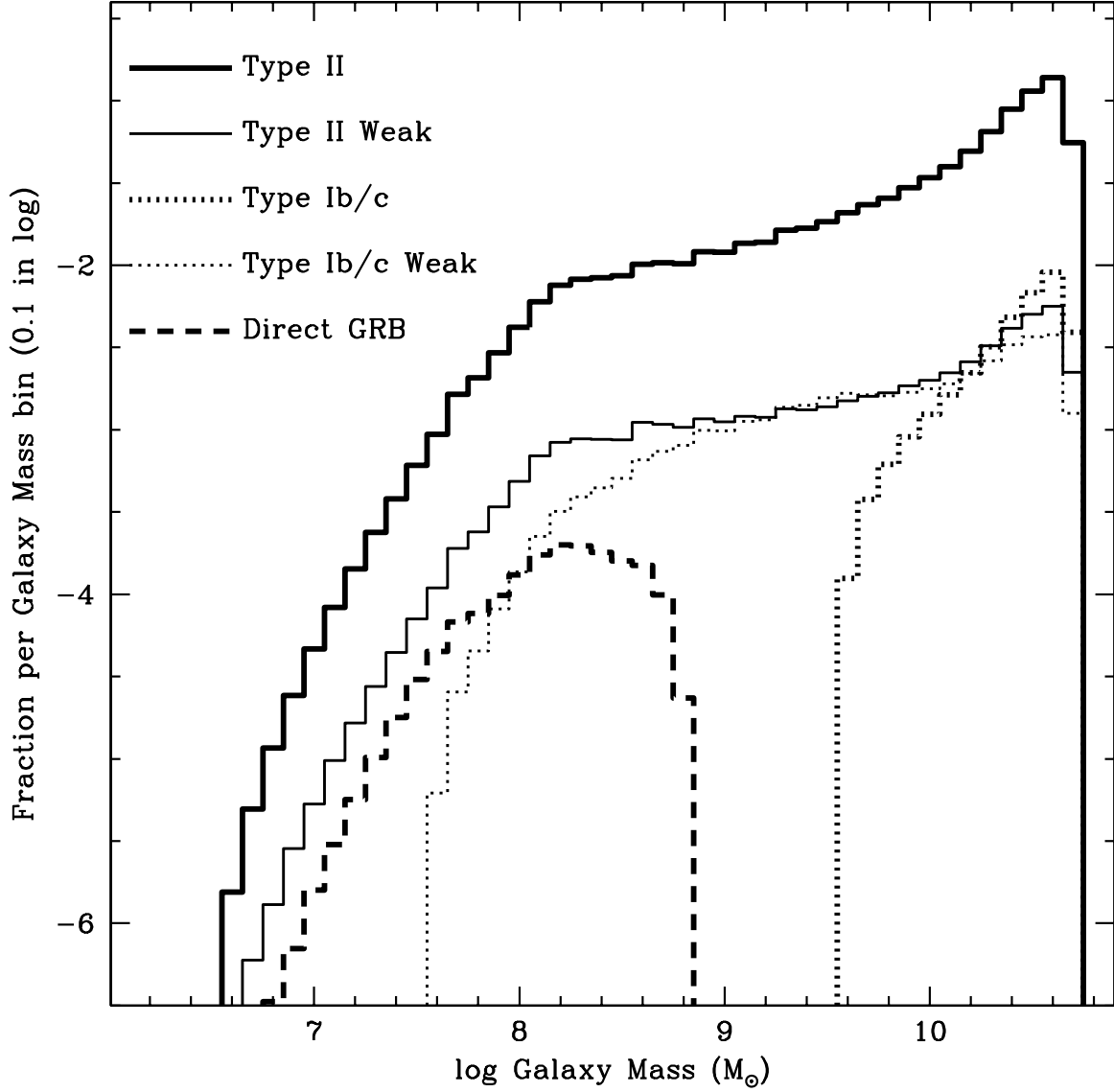


Fig. 5.— Fraction of explosions per galaxy mass bin (0.1 in log space) as a function of metallicity for single stars. The total GRB distribution could be the summation of the direct-collapse and weak Type Ib/c supernovae. Binary systems are nearly identical, except that their distribution could include the direct collapse plus both types of weak supernovae. In any event, it is clear that it could well be that GRBs are produced, preferentially, in smaller mass galaxies.

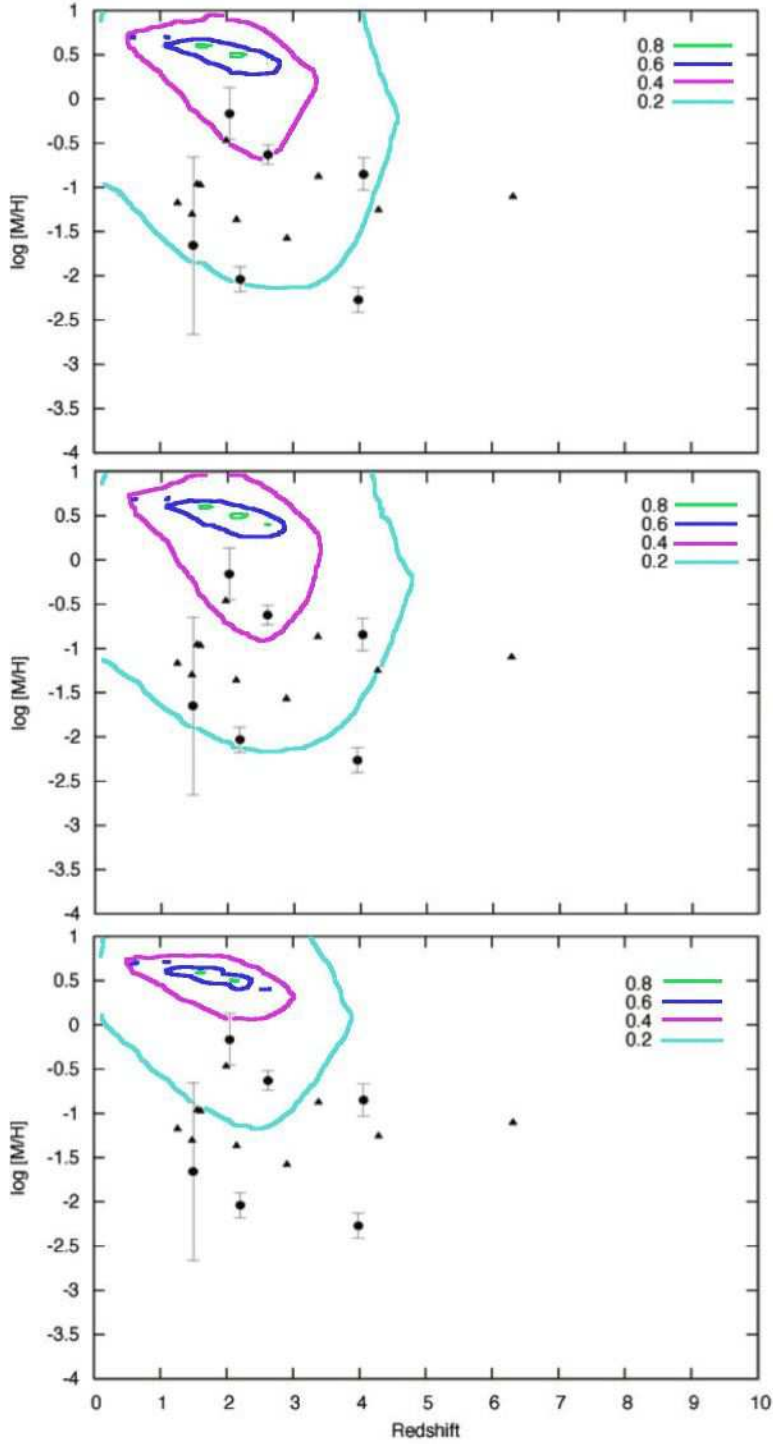


Fig. 6.— Number of binary GRBs including those from weak SN II and Ib/c (top), single star GRBs including weak SN Ib/c (middle), and all supernovae (bottom) per $\Delta = 0.1$ bin in redshift and log metallicity ($\log(z/z_\odot)$), normalized to the number in the peak bin. Contours are plotted for bins with 20, 40, 60, and 80% of the peak number.

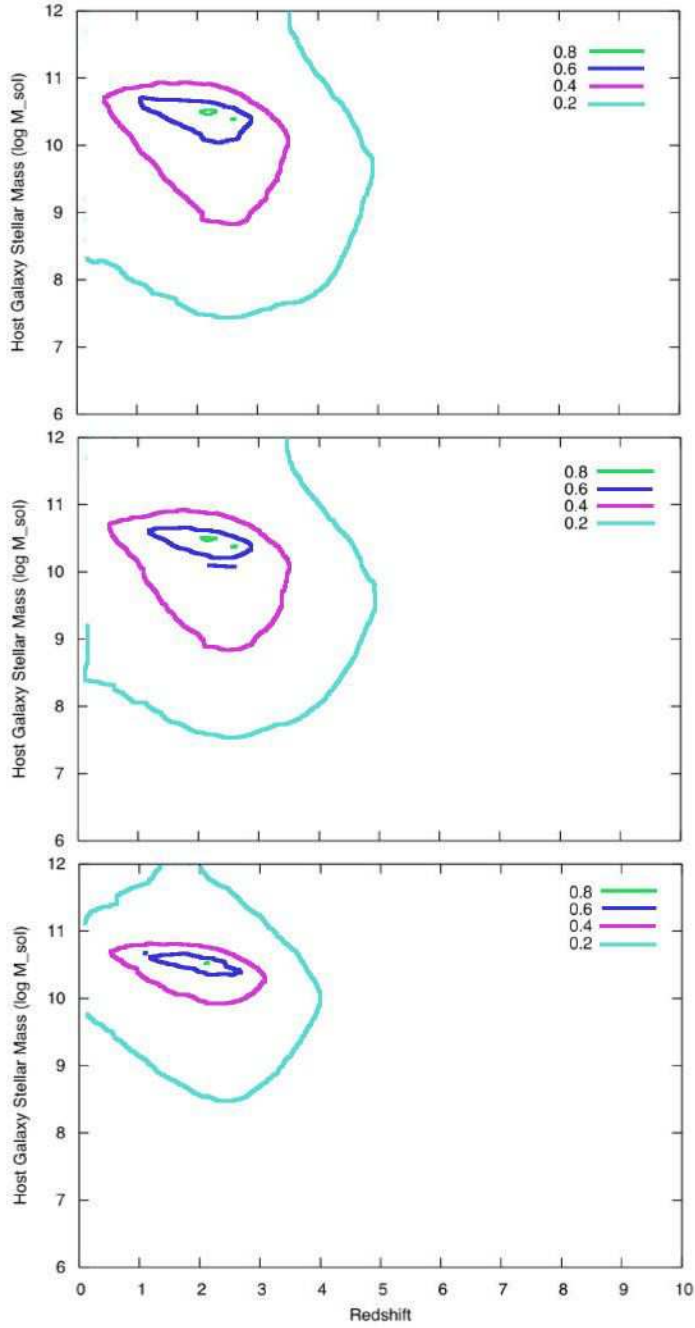


Fig. 7.— Number of binary GRBs including those from weak SN II and Ib/c(top), single star GRBs including weak SN Ib/c (middle), and all supernovae (bottom) per $\Delta = 0.1$ bin in redshift and log of host galaxy stellar mass ($\log(M/M_{\odot})$), normalized to the number in the peak bin. Contours are plotted for bins with 20, 40, 60, and 80% of the peak number.

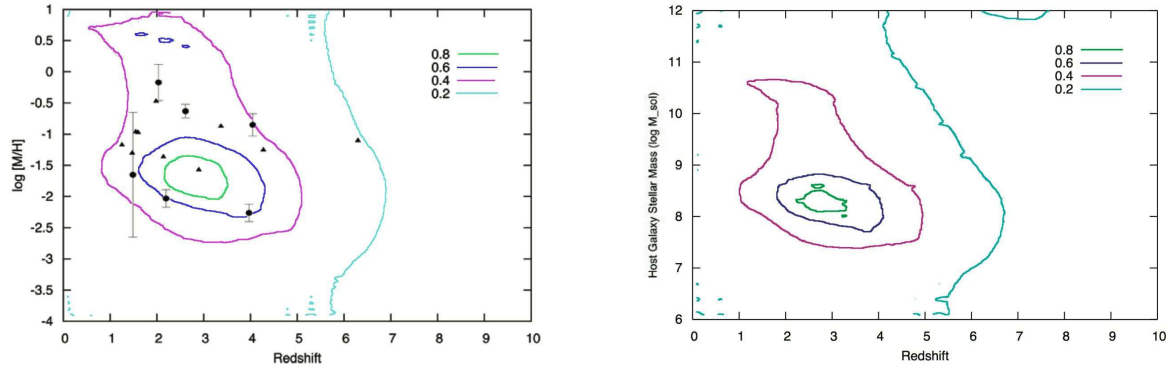


Fig. 8.— Number of single GRBs including those from direct fallback and 2% of weak SN Ib/c per $\Delta = 0.1$ bin in redshift and $\log [M/H]$ (left) and \log of host galaxy stellar mass ($\log(M/M_{\odot})$) (right), normalized to the number in the peak bin. Contours are plotted for bins with 20, 40, 60, and 80% of the peak number. The peaks are at much lower metallicity and host galaxy mass than for scenarios that include all fallback black holes. The observed metallicity distribution also matches better than for all fallback black holes or direct collapse or Yoon & Langer models alone.

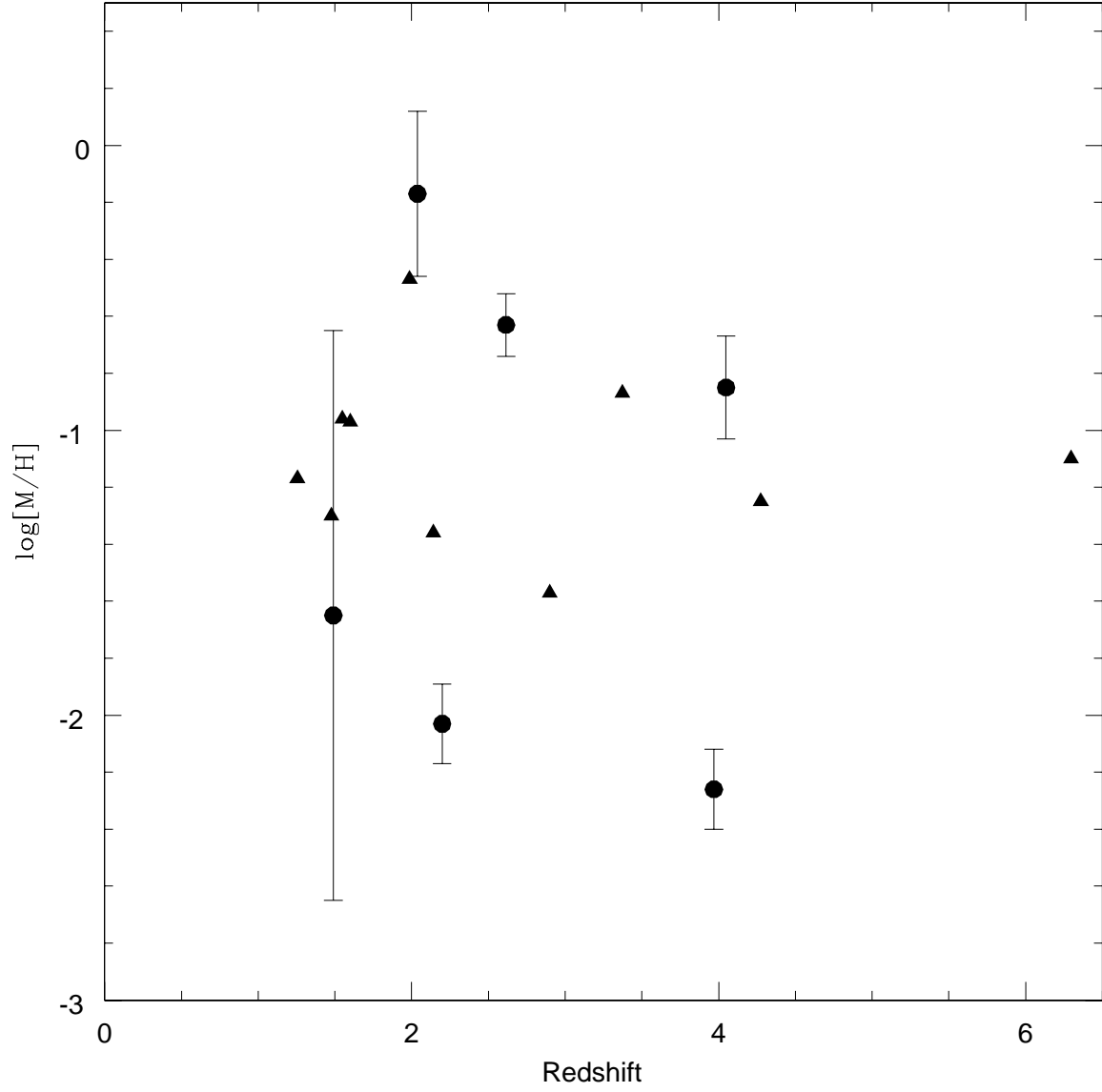


Fig. 9.— Observed metallicity of GRB associated damped $\text{Ly}\alpha$ absorbers versus redshift from the literature (Prochaska 2007). Triangles represent lower limits.